Sensor applications

Dielectric Sensing of Mass Concentration and Moisture in Coal Powders

Thomas Suppan[1] , Markus Neumayer[1]* , Thomas Bretterklieber[1]* , Christoph Feilmayr[2], Stefan Schuster[2]* , and Hannes Wegleiter[1]

[1] Christian Doppler Laboratory for Measurement Systems for Harsh Operating Conditions, Institute of Electrical Measurement and Sensor Systems, Graz University of Technology, A-8010 Graz, Austria
[2] voestalpine Stahl GmbH, A-4040 Linz, Austria
*Member, IEEE

Abstract—In powder processing industries, information about the mass concentration, and the moisture content of the material is often required for process monitoring and control. Capacitive sensors are widely applied for measurements of powder materials, as they are sensitive to variations in mass concentration and changes in moisture content. However, for processes where the mass concentration and the moisture content of the material can vary, it is not possible to distinguish between the two effects based on capacitive measurements alone. This letter shows how permittivity and conductivity measurements can be used to independently determine the mass concentration and the moisture content of a powder. The proposed method is demonstrated for an exemplary coal powder. A dielectric characterization based on impedance measurements of a coaxial probe is carried out. Based on these measurement experiments, a modeling approach is presented that allows the independent determination of the mass concentration and the moisture content of powders, which is of great interest for the development of measurement systems for powder processing industries.

Index Terms—Sensor applications, dielectric mixtures, dielectric sensing, mass concentration, moisture content.

I. INTRODUCTION

Various industrial applications involving the processing of powders require information about the mass concentration β_s and the moisture content x of the material. Examples include flow metering of pneumatically conveyed solids [1], [2], [3] or monitoring fluidized bed reactors [4], [5]. For mass flow measurements in pneumatic conveyors, the mass concentration β_s of the solid particles is a crucial parameter [6], [7], whereas information about the moisture content x of powder materials is needed for monitoring and controlling drying processes in fluidized bed reactors [8], [9].

Electrical measurement methods, such as capacitive sensors, are often used to monitor the processing of powder materials [10], [11], [12]. In capacitive sensing, the measurements are influenced by the dielectric properties of the materials, i.e., the relative permittivity ε_r, which, in turn, depends on the mass concentration β_s as well as on the moisture content x of the powders. The dependence of ε_r on β_s and on x is one of the major drawbacks of capacitive sensors for the application in processes where x and β_s can vary [8], [13]. The determination of the mass concentration of pneumatically conveyed solids is, therefore, prone to error, as the moisture content of the powder varies and the monitoring of drying processes in fluidized bed reactors is affected by fluctuating mass concentrations of the materials [14], [15]. For this reason, a sensing approach capable of determining both the mass concentration and the moisture content of a powdered material is of great interest for the development of instrumentation for powder processing industries.

In this letter, the independent determination of the mass concentration β_s and the moisture content x from permittivity ε_r and conductivity σ measurements of powder materials is proposed. The

dielectric properties of an exemplary coal powder are determined from impedance measurements of a coaxial probe at different mass concentrations and moisture contents. Based on these measurements, a modeling approach of the relationship between the permittivity ε_r, the conductivity σ, the mass concentration β_s, and the moisture content x of the powder material is presented. The developed model can be used to independently determine the mass concentration β_s and the moisture content x from σ and ε_r measurements.

The rest of this letter is organized as follows. In Section II, the measurement setup is discussed. Section III addresses the preparation of the powder samples to generate defined moisture contents. In Section IV, the measurement results are demonstrated and the modeling approach of the relation between σ, ε_r, β_s, and x is discussed. Finally, Section V concludes this letter.

II. MEASUREMENT SETUP

In this section, the measurement setup for the dielectric characterization of powder materials and the determination of the mass concentration is discussed.

A. Dielectric Measurements

The measurement procedure for determining the conductivity σ in $S \cdot m^{-1}$ and the dimensionless relative permittivity ε_r is based on impedance measurements of a coaxial probe [16], [17]. Fig. 1(a) and (b) depicts a sketch and a photo of the coaxial probe, respectively. The main components of the probe are the inner and outer conductors, a base, a cover, an SubMiniature version A (SMA) coaxial connector, and a contact clamp connecting the outer conductor to the shield of the coaxial connection. The radii of the inner and outer conductors are $r_i = 7$ mm and $r_o = 23.5$ mm, respectively. The height of the probe volume is $h = 197.5$ mm. The part of the cover located between the outer and inner conductor has a height of $d = 2.5$ mm, as shown in
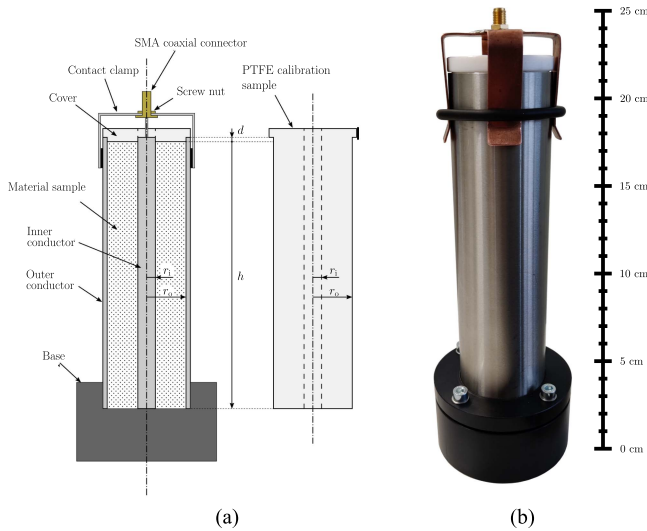
Fig. 1. Coaxial probe for the dielectric characterization of powder materials. (a) Sketch of the coaxial probe and the PTFE sample used for calibration. (b) Photo of the assembled coaxial probe.

Fig. 1(a), and the total length of the conductors is $h + d = 200$ mm. A screw nut fixes the contact clamp, and a polytetrafluoroethylene (PTFE) material sample is used to calibrate the coaxial probe by means of an offset/gain calibration.

Powder materials can be filled between the outer and the inner conductors of the coaxial probe, affecting the probe impedance $\underline{Z}$ in ohms. For the acquisition of the probe impedance, a Rohde & Schwarz ZVL network analyzer is used in this letter. Given the probe impedance $\underline{Z}$, a model-based estimation approach is used to determine σ and ε_r. Details on the probe modeling and the determination of σ and ε_r from the measured probe impedance $\underline{Z}$ can be found in [16] and [17].

B. Generation of Defined Mass Concentrations

To determine the mass concentration of a material sample in the coaxial probe, the mass of the probe filling m_s is determined with a balance [17]. From the mass of the material sample, the mass concentration can be calculated by $\beta_s = m_s/V$, where $V = (r_o^2 - r_i^2)\pi h$ is the volume of the probe. Hereby, it is required that the material sample fills the entire probe volume. To control the mass concentration of the filling, a defined mass of powder m_s is filled into the probe via a funnel, so that the filling height exceeds the height of the probe. Subsequently, the powder is compacted by vibrations, so that the filling height of the powder decreases to $h + d$. Closing the probe with the cover further compacts the powder to the height of the probe volume h. This ensures that the entire probe is filled with the powder material. Repeated measurements with constant mass concentrations show relative standard deviations in the range of 0.1% comparable to the results demonstrated in [17], indicating the repeatability of the measurements. In addition, the measurements were verified by the coaxial probe for fluidized powders, which was demonstrated in [16] and [17]. Hereby, the homogeneity of the material sample is ensured by a fluidization of the powder material by means of an axial gas stream. This approach, however, is limited to relatively dry powders as increased moisture contents disable the homogeneous fluidization of powders due to liquid bridge forces between particles [18]. For moisture contents up to $x = 2\%$, the measurements for fluidized powders agree with measurements carried out for loosely to tightly packed beds of the powder material. Thus, the proposed measurement approach is
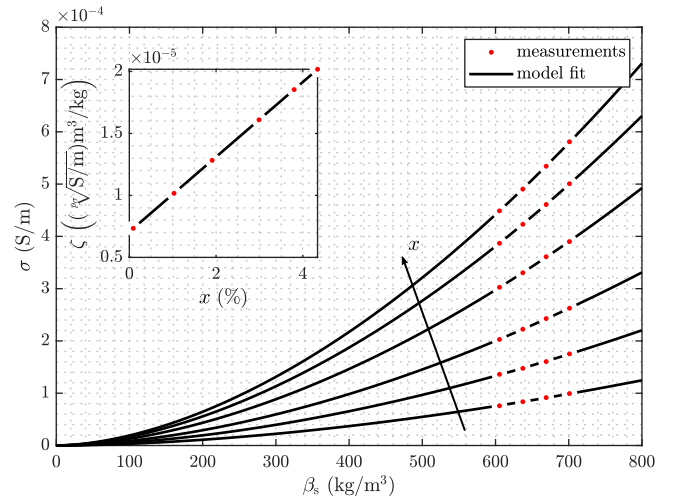

Fig. 2. Conductivity measurements and power model fit with $p_\sigma = 2$ for different moisture contents. In addition, the dependence of the model parameter ζ on the moisture content x is shown.

used to determine σ and ε_r at different mass concentrations β_s [19], [20], [21].

III. PREPARATION OF SAMPLES

This section discusses the preparation of material samples to produce defined moisture contents. The relative moisture content x is defined by

$$x = \frac{m_{\text{water}}}{m_{\text{dry}} + m_{\text{water}}} \tag{1}$$

where m_{dry} is the mass of dry powder, and m_{water} is the mass of water in the material sample. The total mass of a sample is $m_s = m_{\text{dry}} + m_{\text{water}}$. The following procedure is performed to prepare the material samples.

1) The powder samples are filled within saleable containers.
2) Drying of the samples at 105 °C within a climate chamber (fan assisted convection heating) [22], [23], [24].
3) Regularly weighting of the samples. The drying process is completed if $m_s = \text{const.} = m_{\text{dry}}$ (approximately after 72 h).
4) After the drying process is completed, the samples are exposed to an air humidity of >95% at 60 °C within the climate chamber.
5) The weight increase Δm is recorded, which corresponds to the mass of the water $\Delta m = m_{\text{water}}$.
6) The containers are sealed, stored for a week, and turned regularly to obtain a homogeneous moisture distribution.
7) Final weighting of the samples. Moisture content x is calculated according to (1).

IV. MEASUREMENT RESULTS AND MODELING

A. Measurement Results

Figs. 2 and 3 show the conductivity and the relative permittivity of the exemplary coal powder at different mass concentrations β_s and moisture contents x, respectively. The powder has an average particle size of $d_{50} = 30$ μm. The dielectric material properties σ and ε_r are generally frequency dependent. The results shown in Figs. 2 and 3 depict the dielectric material properties at a frequency of $f = 40$ MHz, which corresponds to the operating frequency of a capacitive
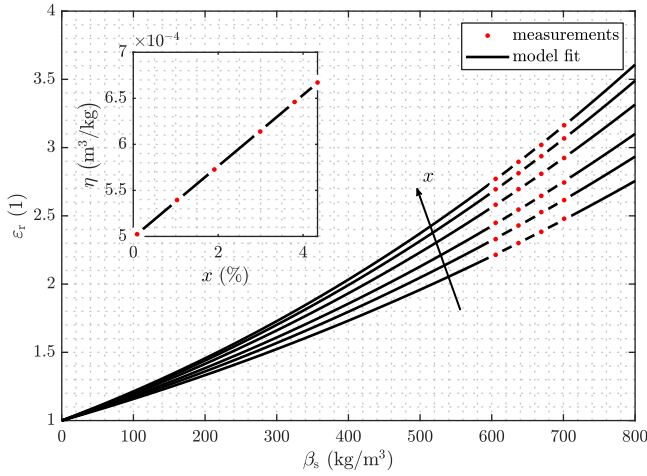
Fig. 3. Permittivity measurements and power model fit with $p_\varepsilon = 3$ for different moisture contents. In addition, the dependence of the model parameter η on the moisture content x is shown.

measurement system used by the authors for flow measurements of pneumatically conveyed solids [6], [10], [25], [26]. However, the results presented in this letter and the applicability of the proposed methods were verified in a frequency range reaching from $f = 1$ MHz to $f = 100$ MHz [16].

Both the conductivity σ and the relative permittivity ε_r increase with increasing mass concentration as well as with increasing moisture content. This stems from the larger ε_r and density values of the solid coal compared to the background material air. This behavior is consistent with the results shown in [17] and [20]. The increase in ε_r and β_s with increasing moisture content x is due to the conductive nature of water and the comparatively high relative permittivity value of $\varepsilon_{r,water} = 80$.

B. Modeling of the Relationship Between σ, ε_r, β_s, and x

To describe the relationship between the dielectric properties of a powder material and the mass concentration, power law models have been successfully applied to a variety of materials [17], [20], [27]. Thus, the relationship between σ and β_s and between ε_r and β_s can be described by

$$\sqrt[p_\sigma]{\sigma} = \zeta(x)\beta_s \tag{2}$$

$$\sqrt[p_\varepsilon]{\varepsilon_r} = \eta(x)\beta_s + 1. \tag{3}$$

In addition to the measurement results, Figs. 2 and 3 also show the power law models fitted to the data. Hereby, $p_\sigma = 2$ and $p_\varepsilon = 3$ resulted in the best fit between the models and the measurements. The values of $p_\sigma = 2$ and $p_\varepsilon = 3$ correspond to the complex refractive index (CRI) mixing equation [28], [29] and the Landau–Lifshitz–Looyenga (LLL) equation [30], [31], respectively [20]. In general, power law models are empirical equations. However, the CRI and LLL equations are physically motivated models that are also valid for mass concentration values below the β_s range of measured values. The model parameters $\zeta(x)$ and $\eta(x)$ are determined from the measurements for each moisture content x. Each moisture content results in different values for $\zeta(x)$ and $\eta(x)$. The relationships between the model parameters and the moisture content x are also depicted in Figs. 2 and 3 showing approximately affine dependencies, i.e., $\zeta = a_0 + a_1x$ and $\eta = b_0 + b_1x$. Substituting these affine approximations for $\zeta(x)$ and
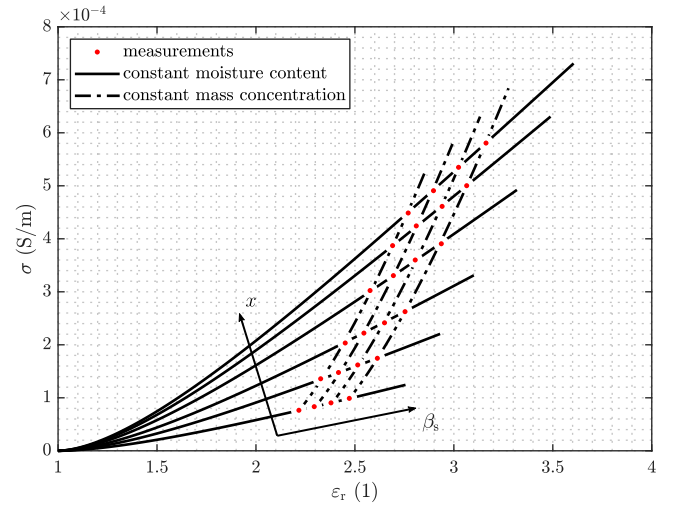

Fig. 4. Conductivity–permittivity plot showing lines of constant moisture and constant mass concentration.
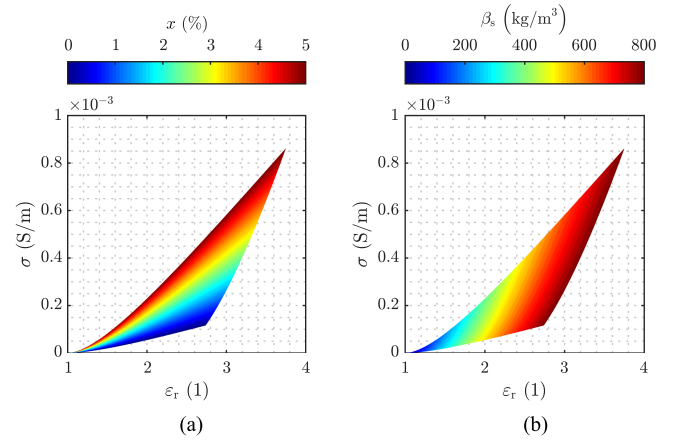

Fig. 5. Illustration of the unique solution of (4) and (5) with respect to the moisture content and the mass concentration. (a) Solution with respect to the moisture content x. (b) Solution with respect to the mass concentration β_s.

$\eta(x)$ into (2) and (3) results in

$$\sqrt[p_\sigma]{\sigma} = (a_0 + a_1x)\beta_s \tag{4}$$

$$\sqrt[p_\varepsilon]{\varepsilon_r} = (b_0 + b_1x)\beta_s + 1. \tag{5}$$

To illustrate that (4) and (5) can be uniquely solved for β_s and x, Fig. 4 depicts σ as a function of ε_r. Hereby, (4) and (5) are evaluated at the mass concentration and moisture content values at which the measurement experiments were performed. This results in contour lines of constant moisture content x and constant mass concentration β_s. Owing to the strictly monotonically increasing behavior of σ and ε_r with respect β_s and x, the contour lines do not overlap, and (4) and (5) can be uniquely solved for β_s and x. The solution of (4) and (5) is illustrated in Fig. 5 showing the unique relationship between a measured σ and ε_r pair and the moisture content x, as well as the mass concentration β_s.

For the demonstration of the proposed method, an exemplary coal powder is used. However, owing to the wide applicability of the LLL equation and the CRI model to various organic materials such as coal,

limestone, flour, corn, bread, etc. [20], [26], [32], [33], [34], the applicability of the proposed measurement approach is not limited to the demonstrated material. The applicability of the affine approximations depicted in Figs. 2 and 3 to describe the relationship between the model parameters η and ζ and the moisture content x has been verified for coal powder for moisture contents up to $x \approx 5\%$. As the ability of organic powders to absorb moisture varies, the relationships $\eta(x)$ and $\zeta(x)$ have to be individually analyzed for different organic powders and moisture content ranges by means of the proposed measurement approach.

V. CONCLUSION

This letter discussed the independent determination of the moisture content and the mass concentration of powder materials based on conductivity and relative permittivity measurements. The dielectric characterization of powders for defined moisture contents and mass concentrations was presented. Based on these measurements, a modeling approach for the relationship between the conductivity, the relative permittivity, the moisture content, and the mass concentration was presented. The derived model allowed the independent determination of the moisture content and the mass concentration of powder materials, making the proposed approach a valuable tool for developing measurement systems for various powder processing industries.

ACKNOWLEDGMENT

REFERENCES

[1] X. Wang, Y. Hu, H. Hu, and L. Li, "Evaluation of the performance of capacitance sensor for concentration measurement of gas/solid particles flow by coupled fields," *IEEE Sens. J.*, vol. 17, no. 12, pp. 3754–3764, Jun. 2017.

[2] A. Hunt, "Weighing without touching: Applying electrical capacitance tomography to mass flowrate measurement in multiphase flows," *Meas. Control*, vol. 47, no. 1, pp. 19–25, 2014.

[3] G. Klinzing, F. Rizk, R. Marcus, and L. Leung, *Pneumatic Conveying of Solids: A Theoretical and Practical Approach*, vol. 3. Dordrecht, The Netherlands: Springer, 2010.

[4] H. Wang and W. Yang, "Application of electrical capacitance tomography in circulating fluidised beds—A review," *Appl. Thermal Eng.*, vol. 176, 2020, Art. no. 115311.

[5] H. Wang and W. Yang, "Application of electrical capacitance tomography in pharmaceutical fluidised beds—A review," *Chem. Eng. Sci.*, vol. 231, 2021, Art. no. 116236.

[6] T. Suppan, M. Neumayer, T. Bretterklieber, S. Puttinger, and H. Wegleiter, "A model-based analysis of capacitive flow metering for pneumatic conveying systems: A comparison between calibration-based and tomographic approaches," *Sensors*, vol. 22, 2022, Art. no. 856.

[7] Y. Yan and D. Stewart, *Guide to the Flow Measurement of Particulate Solids in Pipelines*. London, U.K.: Inst. Meas. Control, Nat. Eng. Lab., Univ. Greenwich, 2001.

[8] J. Zhang, M. Mao, J. Ye, H. Wang, and W. Yang, "Investigation of wetting and drying process in a gas-solid fluidized bed by electrical capacitance tomography and pressure measurement," *Powder Technol.*, vol. 301, pp. 1148–1158, 2016.

[9] M. Aghbashlo, R. Sotudeh-Gharebagh, R. Zarghami, A. S. Mujumdar, and N. Mostoufi, "Measurement techniques to monitor and control fluidization quality in fluidized bed dryers: A review," *Drying Technol.*, vol. 32, no. 9, pp. 1005–1051, 2014.

[10] T. Suppan, M. Neumayer, T. Bretterklieber, S. Puttinger, C. Feilmayr, and H. Wegleiter, "ECT-based mass flow metering in pneumatic conveying processes," in *Proc. 10th World Congr. Ind. Process Tomography*, 2021, pp. 153–158.

[11] W. Zhang, C. Wang, W. Yang, and C.-H. Wang, "Application of electrical capacitance tomography in particulate process measurement—A review," *Adv. Powder Technol.*, vol. 25, no. 1, pp. 174–188, 2014.

[12] L. Baxter, *Capacitive Sensors: Design and Applications* (IEEE Press Series on Electronics Technology), Hoboken, NJ, USA: Wiley, 1996.

[13] W. Yang and H. Wang, "Application of electrical capacitance tomography in pharmaceutical manufacturing processes," in *Proc. IEEE Int. Instrum. Meas. Technol. Conf.*, 2019, pp. 1–6.

[14] M. Samadi, V. Rostampour, and S. Abdollahpour, "A review of solid particles mass flow rate measuring methods: Screening analytic hierarchy process for methods prioritization," *J. Braz. Soc. Mech. Sci. Eng.*, vol. 44, 2022, Art. no. 359.

[15] Y. Zheng and Q. Liu, "Review of certain key issues in indirect measurements of the mass flow rate of solids in pneumatic conveying pipelines," *Measurement*, vol. 43, no. 6, pp. 727–734, 2010.

[16] M. Neumayer, M. Flatscher, and T. Bretterklieber, "Coaxial probe for dielectric measurements of aerated pulverized materials," *IEEE Trans. Instrum. Meas.*, vol. 68, no. 5, pp. 1402–1411, May 2019.

[17] T. Suppan, M. Neumayer, T. Bretterklieber, H. Wegleiter, and S. Puttinger, "Measurement methodology to characterize permittivity-mass concentration relations of aerated bulk materials," in *Proc. IEEE Int. Instrum. Meas. Technol. Conf.*, 2021, pp. 1–6.

[18] T. Yehuda and H. Kalman, "Geldart classification for wet particles," *Powder Technol.*, vol. 362, pp. 288–300, 2020.

[19] S. O. Nelson and S. Trabelsi, "Measurement of grain and seed moisture and density through permittivity relationships," in *Proc. IEEE Instrum. Meas. Technol. Conf. Proc.*, 2010, pp. 964–969.

[20] S. Nelson, "Density-permittivity relationships for powdered and granular materials," *IEEE Trans. Instrum. Meas.*, vol. 54, no. 5, pp. 2033–2040, Oct. 2005.

[21] D. Geldart, "Types of gas fluidization," *Powder Technol.*, vol. 7, no. 5, pp. 285–292, 1973.

[22] L. Fridh, L. Eliasson, and D. Bergström, "Precision and accuracy in moisture content determination of wood fuel chips using a handheld electric capacitance moisture meter," *Silva Fennica*, vol. 52, 2018, Art. no. 1.

[23] P. Ottosson, D. Andersson, and D. Rönnow, "UWB radio measurement and time-domain analysis of anisotropy in wood chips," *IEEE Sens. J.*, vol. 18, no. 22, pp. 9112–9119, Nov. 2018.

[24] P. Pan, T. McDonald, J. Fulton, B. Via, and J. Hung, "Simultaneous moisture content and mass flow measurements in wood chip flows using coupled dielectric and impact sensors," *Sensors*, vol. 17, no. 1, 2017, Art. no. 20.

[25] T. Suppan et al., "Electrical capacitance tomography-based estimation of slug flow parameters in horizontally aligned pneumatic conveyors," *Powder Technol.*, vol. 420, 2023, Art. no. 118418.

[26] T. Suppan, M. Neumayer, T. Bretterklieber, and H. Wegleiter, "Thermal drifts of capacitive flow meters: Analysis of effects and model-based compensation," *IEEE Trans. Instrum. Meas.*, vol. 70, 2021, Art. no. 4501311.

[27] B. Hadi, F. Berruti, and C. Briens, "New calibration methods for accurate electrical capacitance tomography measurements in particulate-fluid systems," *Ind. Eng. Chem. Res.*, vol. 48, pp. 274–280, 2008.

[28] A. Kraszewski, "Prediction of the dielectric properties of two-phase mixtures:," *J. Microw. Power*, vol. 12, pp. 215–222, 1977.

[29] J. R. Birchak, C. G. Gardner, J. E. Hipp, and J. M. Victor, "High dielectric constant microwave probes for sensing soil moisture," *Proc. IEEE*, vol. 62, no. 1, pp. 93–98, Jan. 1974.

[30] D. C. Dube, "Study of Landau-Lifshitz-Looyengas formula for dielectric correlation between powder and bulk," *J. Phys. D, Appl. Phys.*, vol. 3, pp. 1648–1652, 1970.

[31] H. Looyenga, "Dielectric constants of heterogeneous mixtures," *Physica*, vol. 31, pp. 401–406, Mar. 1965.

[32] S. Nelson, "Permittivity and density relationships for granular and powdered materials," in *Proc. IEEE Antennas Propag. Soc. Symp.*, 2004, pp. 229–232.

[33] B. Gillay and D. Funk, "Efficacy of the Landau-Lifshitz, Looyenga mixture equation for density-correcting dielectric measurements of yellow-dent corn subjected to vibration and pressure," in Proc. ASAE Annu. Meeting, 2002, Art. no. 026038.

[34] Y. Liu, J. Tang, and Z. Mao, "Analysis of bread dielectric properties using mixture equations," *J. Food Eng.*, vol. 93, no. 1, pp. 72–79, 2009.